Hong Kong J Radiol. 2013;16:110-6 | DOI: 10.12809/hkjr1313167

ORIGINAL ARTICLE

Cone-beam Computed Tomography of the Paranasal Sinuses: Comparison Study with Multidetector Computed Tomography

PL Kei[1], JSP Tan[1], JL Leong[2], YM Kwok[1], WEH Lim[1], LL Chan[1]

[1]Department of Diagnostic Radiology, and [2]Department of Otolaryngology, Singapore General Hospital, Outram Road, Singapore 169608

ABSTRACT

Objectives: *Cone-beam computed tomography (CBCT) in sinonasal imaging is fairly novel and remains limited to date. This study aimed to compare (1) the image quality of CBCT and multidetector computed tomography (MDCT), and (2) the eye lens dose for paranasal sinus imaging between these two modes of imaging.*

Methods: *This study was approved by an institutional ethics review board. Sixteen patients underwent CT imaging of their paranasal sinuses for the evaluation of chronic rhinosinusitis using both CBCT and MDCT. The eye lens dose was measured using lithium fluoride thermoluminescent dosimeters during each scan. The scans were read independently by two readers for the presence of sinonasal opacification, artefacts, clarity of osseous structures and soft tissues (based on 5-point grading scales). The interclass coefficient was used to assess interobserver variability.*

Results: *The mean eye lens dose was 1.0 mGy on CBCT and 1.4 mGy on MDCT. Respective grading scores for opacification, artefacts, osseous structures, and soft tissues were 4.3, 3.9, 4.0 and 2.0 on CBCT compared with 4.2, 4.3, 4.6 and 4.2 on MDCT. Score differences between CBCT and MDCT for artefacts, osseous structures, and soft tissues were statistically significant ($p < 0.05$).*

Conclusion: *The image quality of CBCT scans was generally inferior, but adequate for screening purposes in the assessment of opacification and osseous detail. Compared with MDCT scans, the mean eye lens dose with CBCT was also lowered by 25%.*

Key Words: *Cone-beam computed tomography; Image enhancement; Paranasal sinuses; Radiation dosage*

中文摘要

副鼻竇的錐形束CT與多排螺旋CT的比較研究

葛炳林、陳淑萍、梁任靈、郭耀文、林永豪、曾玲玲

目的：鼻腔鼻竇的錐形束CT（CBCT）成像相當新穎，至今仍未普及。本研究旨在比較CBCT和多排螺旋CT（MDCT）兩種方式的圖像質素以及鼻竇成像中眼晶狀體所受輻射劑量。

方法：本研究已獲機構審查委員會批准。16名慢性鼻竇炎患者同時接受CBCT和MDCT副鼻竇CT掃描。每次掃描過程中都會使用氟化鋰熱釋光劑量儀測定眼晶狀體的輻射劑量。掃描結果由兩位醫生獨立閱片，評估鼻竇渾濁化、偽影、骨性結構和軟組織的清晰度（按5點分級表）。以組間相關系數

Correspondence: *Dr Pin-Lin Kei, Department of Diagnostic Radiology, Singapore General Hospital, Outram Road, Singapore 169608.*
Tel: (65) 6326 6203; Fax: (65) 6326 5242; Email: kei.pin.lin@sgh.com.sg

Submitted: 28 Jan 2013; Accepted: 13 Mar 2013.

來評估評分者之間的差異。

結果：CBCT的眼晶狀體平均輻射劑量為1.0 mGy，而MDCT則為1.4 mGy。至於鼻竇渾濁化、偽影、骨性結構和軟組織的清晰度，CBCT的評分分別為4.3、3.9、4.0和2.0，MDCT則分別為4.2、4.3、4.6和4.2。CBCT和MDCT在偽影、骨性結構和軟組織的清晰度分數差異達統計學意義（$p < 0.05$）。

結論：CBCT掃描成像的質素普遍較低，但尚可勝任評估渾濁化和細微骨性結構。與MDCT掃描相比，CBCT的眼晶狀體平均輻射劑量降低了25%。

INTRODUCTION

Cone-beam computed tomography (CBCT) is a popular modality used in dentomaxillofacial imaging.[1] In recent years, pilot studies have also explored the use of this technology in imaging of other body parts.[2,3] The technique utilises a cone-shaped X-ray beam and a two-dimensional (2D) flat-panel detector system in a single 180º or 360º gantry rotation[4] to produce true 3D images with isotropic resolution of 0.4 mm or less (range, 0.4-0.125 mm).[1] Compared with conventional CT machines, CBCT machines are much smaller, more compact, and suitable for office use. When new large field of view (FOV) CBCT machines came into the market, it becomes possible for ear, nose and throat (ENT) specialists to locate such units for low patient radiation dose screening in their small / confined office spaces. This can facilitate patient assessment for common otorhinolaryngological disorders such as chronic rhinosinusitis (CRS). If feasible, office CBCT could augment the diagnostic work-up of such patients, particularly those suffering from atypical symptoms of CRS as early diagnosis or exclusion of the disease can avoid unnecessary recourse to long-term steroids and antibiotics.

To date, use of CBCT in sinonasal imaging remains fairly limited. To our knowledge, no clinical study has compared its utility with conventional CT scanners for sinonasal imaging. In addition, although the technique has been reported to result in reduced radiation in dentomaxillofacial applications based on phantom studies,[5] its application in clinical sinonasal imaging is still unclear. This prospective clinical study therefore aimed to compare (1) sinonasal imaging quality with CBCT and multidetector computed tomography (MDCT), and (2) the eye lens dose obtained for paranasal imaging with these two imaging modalities.

METHODS

Approval for this study was obtained from the Institutional Ethics Review Board of the Singapore General Hospital and informed consent was obtained from all patients prior to imaging. Institutional Ethics Review Board approval was conditional on ensuring a low radiation dose and obtaining informed consent form prior to imaging from every patient.

Patient Data

Patients with symptoms of CRS referred from the ENT clinic for imaging of the paranasal sinuses over a 3-month period from June to August 2008 were invited to participate in this study. Children and young patients below the age of 21 years were excluded. Sixteen patients (8 men and 8 women) were recruited and first underwent MDCT followed immediately by CBCT of the paranasal sinuses on the same day. All 16 patients had had a trial of medical therapy (≥3 months) and were being followed up for persistent symptoms of CRS. Their ages ranged from 24 to 69 years (mean, 46 years).

The MDCT scans were acquired on a 64-slice dual-source machine (SOMATOM Definition, Siemens, Germany). For the purpose of this study, the dual-source MDCT was utilised in a single source mode and hence its performance was essentially the same as that of a 64-slice MDCT. We followed our institution's standard clinical protocol for imaging the paranasal sinuses: supine, single-source spiral mode, 120 kV, 80 mA, 0.6 mm slice collimation, pitch factor 0.9 with a rotation time of 0.33 s, and automatic tube current modulation with a FOV ranging from 130 x 110 mm to 170 x 120 mm. Contiguous 3 mm coronal and axial sections were reconstructed from the image datasets with a B70f sharp / bone kernel.

Immediately after MDCT, each patient had their second scans with the CBCT machine. This protocol was needed as the ENT surgeons were keen on a 'like-for-like' comparison in image quality and radiation dose.

The CBCT scans were acquired on the 3D Accuitomo XYZ machine (J. Morita Corporation, Kyoto, Japan)

using a limited range of 80-90 kV and 5-6 mA based on the manufacturer's recommendations. The patient sat upright, with the jaw resting on the chin rest during a 17.5-second exposure, using a 360° gantry rotation. The FOV was fixed at the maximum of 170 x 120 mm, so as to ensure adequate coverage of the paranasal sinuses. True 3D images with an isotropic resolution of 0.125 mm were produced, and were reconstructed into coronal and axial CBCT images at a preset slice width of 3.3 mm (the lowest allowable on the CBCT machine), to match the sections obtained on the MDCT (3.0 mm) as closely as possible.

Image Quality

All scans were independently evaluated by two experienced radiologists (>10 and >2 years), with expertise in sinonasal imaging. The image sets (in both coronal and axial planes) were presented together in a random fashion and the readers were blinded to the relevant parametric data. The MDCT images were viewed on a clinical Siemens reporting workstation with a display matrix 512 x 512, using a fixed window level of 700 HU and width of 3500 HU for bone structures, and window level of 50 HU and width of 350 HU for soft tissues. The CBCT images were viewed using the custom-made software, iDixel (J. Morita corporation), with a display matrix of 512 x 512 and default bone settings of Gray level 0-255 and Data level 0-255, and soft tissue settings of Gray level 0-255 and Data level 30-255.

Image quality was assessed using a modified 5-point Bernhardt's grading scale[6,7] for a total of 22 criteria in the following groups:

(1) Opacification: the paranasal sinuses (including frontal, ethmoidal, sphenoidal and maxillary), and nasal cavities graded as a whole unit (1 criterion);
(2) Artefacts: beam hardening artefacts (including dental amalgam streak artefacts) [1 criterion];
(3) Osseous structures: clarity of the infra-orbital canal, medial orbital wall, medial maxillary sinus wall, uncinate process, middle turbinate, ethmoidal septa, and fovae ethmoidalis / cribriform plate (14 criteria, including left and right sides[6]); and
(4) Soft tissue structures: clarity of medial rectus muscles, optic nerves, and ventricular frontal horns (6 criteria, including left and right sides[7]).

The grading for opacification ranged from 1 to 5:

- Grade 1: sinonasal cavity completely opacified;
- Grade 2: more than 75% opacification;
- Grade 3: more than 50% opacification;
- Grade 4: more than 25% opacification;
- Grade 5: no to 25% opacification.

For the other three groups, the 5-point grading scale used comprised:

- Grade 1: unacceptable images — not suitable for screening purposes;
- Grade 2: poor images resulting in uncertainty for screening purposes;
- Grade 3: Adequate image quality, with the correct diagnosis being highly likely;
- Grade 4: good images, enabling a confident diagnosis;
- Grade 5: excellent images of best diagnostic value.

We considered an image quality of Grade 3 or higher as adequate for screening purposes. The scores obtained by both modalities (for coronal and axial planes) were summated and analysed.

Dosimetry

All LiF:Mg,Ti (thermoluminescent dosimeter [TLD]-100) dosimeters were calibrated to a known dose of 100 mGy with a 6 Mv X-ray photon beam medical linear accelerator (Clinac 2100 Ex;Varian Medical Systems, Palo Alto [CA], USA). As the lens is a superficial organ located 6-8 mm below the skin surface, we assume the entrance dose to be equal to the eye lens dose. Two TLDs per eye were placed over the eyelids of the patients during each scan, yielding a total of 4 TLDs per scan or 8 TLDs per patient. Following irradiation, the dosimeters were readout on a Harshaw 3500 (Thermo Fisher Scientific, Waltham [MA], USA) to determine the unknown entrance surface dose received for each scan protocol. The variation in sensitivity of the TLD batches was calculated. The energy responses of the TLDs at the energy range for MDCT and CBCT were accounted for in the measurements.[8-10]

Statistical Analysis

A pooled analysis was performed by combining the two readers' gradings. Differences in image quality between scans acquired by MDCT and CBCT were compared using the Wilcoxon signed rank test. Significance was defined at $p < 0.05$. The impact of the degree of opacification on the grading score of the osseous structures was determined using Spearman's correlation. Interobserver variability in image quality assessment was calculated using the interclass correlation coefficient (r).

RESULTS

Patient demographics, degree of sinonasal opacification, image quality grading, and dosimetrics for the MDCT and CBCT scans are summarised in Tables 1 to 3. The majority (12/16, 75%) of the patients in our study had minor (Grade 4, 10 patients) or no (Grade 5, 2 patients) sinonasal opacification (Table 1). Dosimetric measurement showed a lower mean eye lens dose obtained on CBCT than on MDCT by 25% (Table 2). Qualitative analysis of the images showed no significant difference in the image grading for the degree of opacification ($p > 0.05$); whilst the quality of the images for screening purposes obtained on CBCT were significantly lower than those from MDCT scans for all the other three groups of criteria ($p < 0.05$; Table 3). Spearman analysis showed a positive correlation between more extensive opacification of the paranasal sinuses and poorer image quality grading, this being true for both CBCT ($r = 0.601$) and MDCT ($r = 0.651$).

A review of the scans showed a more pronounced beam-hardening effect on CBCT scans as compared with MDCT scans, especially at interfaces of the bone and soft tissues (Figures 1a, 1b). Streak artefacts around the dental amalgam were present on both CBCT and MDCT scans. However, beam-hardening effect deep to the zygomas was a feature seen only on CBCT scans (Figure 1a). On CBCT scans, motion artefacts, whilst not gross, were sometimes seen as subtle blurring at the bony margins (Figure 1b). These artefacts did not interfere with interpretation of the pool of images in our study (adequate image quality score of Grade 3 and above; Table 3). MDCT images generally yielded excellent bony details, especially in the absence of significant opacification (Figures 1c to 1f). The bony

Table 1. Patient demographics and degree of sinonasal opacification (n=16).

Demographics	Data
Mean (± standard deviation) age (years)	45.6 ± 15.38
Gender	
Male	8 (50%)
Female	8 (50%)
Sinonasal opacification	
Grade 1 (>complete)	1 (6%)
Grade 2 (>75%)	1 (6%)
Grade 3 (>50%)	2 (13%)
Grade 4 (>25%)	10 (63%)
Grade 5 (no to 25%)	2 (13%)

Table 3. Image quality assessment between sinonasal scans performed on CBCT and MDCT.*

Image quality	CBCT	MDCT	p Value
Opacification (1 criterion)	4.27 ± 1.15	4.22 ± 1.17	0.763
Artefact (1 criterion)	3.94 ± 0.25	4.31 ± 0.47	<0.05
Osseous (14 criteria)	3.96 ± 0.90	4.57 ± 0.68	<0.0001
Soft tissue (6 criteria)	2.00 ± 0.86	4.21 ± 0.79	<0.0001

Abbreviations: CBCT = cone-beam computed tomography; MDCT = multidetector computed tomography.

* Comparison was made between the image quality scores of the two different CT scanners using Wilcoxon signed rank test; statistical significance was defined at $p < 0.05$.

Table 2. Respective scan protocols and eye lens dose of CBCT and MDCT imaging.

Patient No.	Effective current (mA)		Tube voltage (kVp)		CTDIvol (mGy)		DLP (mGy.cm)		Eye lens dose (mGy)	
	CBCT	MDCT	CBCT	MDCT	CBCT	MDCT	CBCT	MDCT	CBCT	MDCT
1	6	80	90	120	9.60	12.00	115.00	173.00	1.37 ± 0.05	1.31 ± 0.02
2	6	80	90	120	9.60	12.00	115.00	166.00	1.43 ± 0.09	1.34 ± 0.11
3	6	80	90	120	9.60	12.00	115.00	203.00	1.20 ± 0.02	1.36 ± 0.02
4	5	80	90	120	8.10	12.00	97.00	228.00	0.99 ± 0.02	1.34 ± 0.08
5	5	80	90	120	8.10	12.00	97.00	170.00	1.21 ± 0.05	1.31 ± 0.06
6	5	80	90	120	8.10	12.00	97.00	170.00	0.97 ± 0.02	1.55 ± 0.01
7	5	80	80	120	5.90	12.00	71.00	161.00	0.80 ± 0.02	1.41 ± 0.05
8	5	80	80	120	5.90	12.00	71.00	178.00	0.82 ± 0.01	1.40 ± 0.06
9	5	80	80	120	5.90	12.00	71.00	191.00	0.81 ± 0.00	1.35 ± 0.08
10	5	80	80	120	5.90	12.00	71.00	196.00	0.92 ± 0.05	1.38 ± 0.04
11	5	80	85	120	5.90	12.00	71.00	180.00	1.05 ± 0.08	1.49 ± 0.06
12	5	80	85	120	5.90	12.00	71.00	180.00	1.01 ± 0.00	1.34 ± 0.02
13	5	80	85	120	5.90	12.00	71.00	172.00	0.89 ± 0.00	1.40 ± 0.08
14	5	80	80	120	5.90	12.00	71.00	170.00	0.96 ± 0.04	1.33 ± 0.03
15	5	80	80	120	5.90	11.80	71.00	192.00	1.05 ± 0.03	1.38 ± 0.00
16	5	80	80	120	5.90	12.00	71.00	201.00	1.04 ± 0.03	1.54 ± 0.02
Overall	-	-	-	-	-	-	-	-	1.03 ± 0.17	1.38 ± 0.08

Abbreviations: CBCT = cone-beam computed tomography; MDCT = multidetector computed tomography; CTDI = CT dose index; DLP = dose-length product.

details evident on CBCT images were generally worse, but still adequate for screening purposes (Table 3). In cases when there was significant sinonasal disease opacifying the sinuses, visualisation of the fine bony details suffered in both MDCT and CBCT images, and sometimes far worse with the latter (Figures 1g, 1h).

	CBCT	MDCT	Description
a	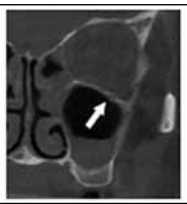		Infra-orbital canal graded as 3 on CBCT and 5 on MDCT in patient No. 7. The superior and inferior walls of the left infra-orbital canal are slightly blurred due to beam-hardening effect from the zygoma on CBCT, but clearly depicted on MDCT.
b	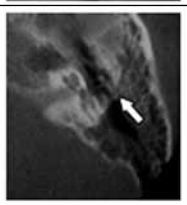	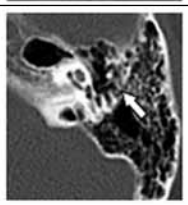	Temporal bone graded as 3 on CBCT and 5 on MDCT in patient No. 7. The mastoid bony septae are unclear due to combination of beam hardening from the surrounding dense bones, and motion artefacts on CBCT, as compared with the clear images on MDCT.
c	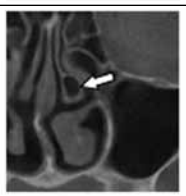	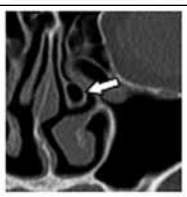	Middle turbinate graded as 4 on CBCT and 5 on MDCT in patient No. 9. The bony details are clear on both CBCT and MDCT, when the paranasal sinuses are free from mucosal disease.
d	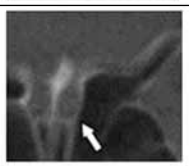	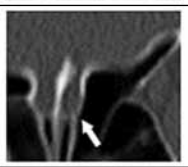	Fovea ethmoidalis / cribriform plate graded as 4 on CBCT and 5 on MDCT in patient No. 9.
e	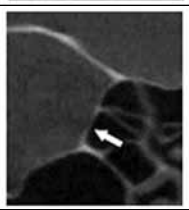		Medial orbital wall graded as 5 on CBCT and 5 on MDCT in patient No. 5.
f	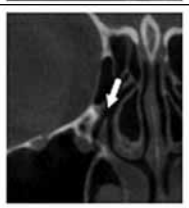	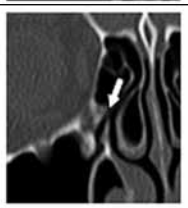	Medial maxillary sinus wall / uncinate process graded as 5 on CBCT and 5 on MDCT in patient No. 2. Excellent bony details on both CBCT and MDCT are seen when the paranasal sinuses are free from mucosal disease.
g	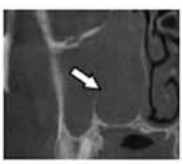		Uncinate process / medial wall of the right maxillary sinus, graded as 2 on CBCT and 3 on MDCT in patient No. 8. There is a suggestion of demineralisation of the medial wall of the right maxillary sinus and uncinate process on CBCT. Whilst the edge of the demineralised wall is well seen on MDCT, note that structures in the right nasal cavity are also demineralised by nasal polyposis.
h			Ethmoid septae graded as 2 on CBCT and 3 on MDCT in patient No. 8. There is a suggestion of demineralisation on CBCT, but the bony septa is clearly seen on the MDCT without evidence of demineralisation.

Figure 1. Images of the osseous structures in different patients obtained by cone-beam computed tomography (CBCT) and multidetector computed tomography (MDCT) scanners: (a) infra-orbital canal, (b) temporal bone, (c) middle turbinate, (d) fovea ethmoidalis, (e) medial orbital wall, (f) medial maxillary sinus wall, (g) uncinate process, and (h) ethmoid septae.

	CBCT	MDCT	Description
a			Medial rectus muscles and optic nerves graded as 2 on CBCT and 4 on MDCT. Poor soft tissue depiction on CBCT compared with MDCT.
b		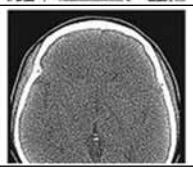	Ventricle graded as 1 on CBCT. The MDCT was graded as 4. Soft tissue visualisation was significantly worse on CBCT, compared with MDCT. For example, comparing the ventricular frontal horns between the two modalities.

Figure 2. Images of the soft tissue structures obtained in patient No. 9 by cone-beam computed tomography (CBCT) and multidetector computed tomography (MDCT) scanners: (a) medial rectus muscles and optic nerves, and (b) ventricular frontal horns.

Soft tissues visualisation was also significantly worse on CBCT, resulting in diagnostic uncertainty (Figure 2). In contrast, visualisation of the soft tissues on MDCT remained clear and allowed confident diagnosis even though the images were processed on a bone algorithm (Table 3).

DISCUSSION

Opacification and osseous detail are of chief interest in sinonasal imaging. In our study, although sinonasal opacification on CBCT compared favourably with MDCT, using the manufacturer's recommended tube settings the image quality of the scans obtained were generally inferior to our MDCT images. In this study, bony assessment was graded worse with CBCT than MDCT images. Poorer depiction of soft tissues by CBCT also resulted in diagnostic uncertainty. This too was a drawback, as soft tissue assessment constitutes an important aspect routinely surveyed and reported by radiologist with respect to disease complications or coincidental abnormalities that clinically mimics CRS symptoms.

The degradation of image quality in CBCT[10,11] was mainly due to the geometry of the cone beam (large beam angle and FOV) that drastically increased radiation scatter and decreased the contrast-to-noise ratio. The low tube current CBCT used in our study and the lack of an anti-scatter grid for the flat screen detector further contributed to the noise. As a result, the visualisation of soft tissues on CBCT images was significantly impaired due to the scatter, noise, limited temporal resolution, and dynamic range of the flat panel detector as compared with those on the MDCT. Hence, the use of CBCT for the head and neck is best reserved for pathology in regions where there is good inherent contrast, such as dental and sinonasal areas where natural air-bone interfaces exist in abundance.

Other reported potential contributors to image degradation with CBCT include 'streaks' from beam hardening of dental amalgam and beneath the zygoma (Figures 1a, 1b) and 'cupping' artefacts (reduced voxel values near the centre of an image),[12] but in our experience these artefacts did not interfere with diagnostic assessment. In contrast to the more immobile supine positions used for MDCT scans, the CBCT scans are more susceptible to motion artefacts as the patient is in an erect or sitting position and the gantry rotation speed is slower.[10]

In this clinical study, the CBCT machine delivers a lower radiation dose to the eye compared with the MDCT scans[13] for several reasons. One reason is that as opposed to the multiple stack images acquired by the latter, those acquired on the 2D CBCT detector are obtained in a single revolution of the radiation source around the entire region of interest. Other reasons include a lower current used in CBCT than MDCT.

In our study, the relative good quality of osseous detail with CBCT (mean grade of 3.96; Table 3) was partly contributed by the superior resolution offered by isotropic data acquisition and flat panel technology.[10,11] Furthermore, the spatial resolution of our CBCT (0.125 mm) was superior to that from MDCT (0.33 mm). In addition, the majority of the patients in our study (12/16, 75%) had minor or no disease. The presence of sinonasal mucosal disease is known to affect the density of the bony architecture of the paranasal sinuses, which in turn may adversely affect the image quality.[14,15] In a screening referral base largely comprised of

patients with minor sinonasal disease (as in our study group), CBCT may be adequate and effective in depicting disease and reducing the eye lens. However, commenting on the efficacy of CBCT in pre-surgical road mapping for patients with significant sinonasal disease is beyond the scope of this study.

Our study was limited by the small sample size of recruited patients. A distinct advantage of our 3D Accuitomo XYZ CBCT machine was its small size, enabling its use in a confined office space. In view of the scarcity of clinical dosimetric data in the literature, we believe our results provide some insights into the utility of CBCT in clinical sinonasal imaging.

In conclusion, CBCT of the paranasal sinuses produces images that are adequate for screening purposes, for the assessment of opacification and osseous detail in our patient group. Using the clinical parameters mentioned in this study, the eye lens dose in this CBCT machine was lower than that encountered with our current MDCT machine clinical protocol. However, soft tissue assessment remains suboptimal with CBCT imaging, particularly when compared with MDCT and therefore leads to diagnostic uncertainty.

ACKNOWLEDGEMENTS

We wish to thank the Head of Diagnostic Radiology and surgeons of the Ear-Nose-Throat (ENT) Department for their support in this study, the technologist Lydia Tan Kheng Lui and Muhammad Illyas for performing the scans, and our research coordinators Doreen Lau and Ching-Ming Wan, for their assistance in the preparation of this manuscript, database management, and statistical analysis.

DECLARATION

No conflict of interests were declared by authors.

REFERENCES

1. Kau CH, Richmond S, Palomo JM, Hans MG. Three-dimensional cone beam computerized tomography in orthodontics. J Orthod. 2005;32:282-93. cross ref
2. Yang WT, Carkaci S, Chen L, Lai CJ, Sahin A, Whitman GJ, et al. Dedicated cone-beam breast CT: feasibility study with surgical mastectomy specimens. AJR Am J Roentgenol. 2007;189:1312-5. cross ref
3. Orth RC, Wallace MJ, Kuo MD; Technology Assessment Committee of the Society of Interventional Radiology. C-arm cone-beam CT: general principles and technical considerations for use in interventional radiology. J Vasc Interv Radiol. 2008;19:814-20. cross ref
4. Jaffray DA, Siewerdsen JH. Cone-beam computed tomography with a flat-panel imager: initial performance characterization. Med Phys. 2000;27:1311-23. cross ref
5. Ishikura R, Ando K, Nagami Y, Yamamoto S, Miura K, Pande AR, et al. Evaluation of vascular supply with conebeam computed tomography during intraarterial chemotherapy for a skull. Radiat Med. 2006;24:384-7. cross ref
6. Bernhardt TM, Rapp-Bernhardt U, Fessel A, Ludwig K, Reichel G, Grote R. CT scanning of the paranasal sinuses: axial helical CT with reconstruction in the coronal direction versus coronal helical CT. Br J Radiol. 1998;71:846-51.
7. Brem MH, Zamani AA, Riva R, Zou KH, Rumboldt Z, Hennig FF, et al. Multidetector CT of the paranasal sinus: potential for radiation dose reduction. Radiology. 2007;243:847-52. cross ref
8. Davis SD, Ross CK, Mobit PN, Van der Zwan L, Chase WJ, Shortt KR. The response of lif thermoluminescence dosemeters to photon beams in the energy range from 30 kV x rays to 60Co gamma rays. Radiat Prot Dosimetry. 2003;106:33-43. cross ref
9. McNitt-Gray MF. AAPM/RSNA Physics tutorial for residents: Topics in CT. Radiation dose in CT. Radiographics. 2002;22:1541-53. cross ref
10. Orth RC, Wallace MJ, Kuo MD; Technology Assessment Committee of the Society of Interventional Radiology. C-arm cone-beam CT: general principles and technical considerations for use in interventional radiology. J Vasc Interv Radiol. 2008;19:814-20. cross ref
11. Miracle AC, Mukherji SK. Conebeam CT of the head and neck, part 2: clinical applications. AJNR Am J Neuroradiol. 2009;30:1285-92. cross ref
12. Siewerdsen JH, Jaffray DA. Cone-beam computed tomography with a flatpanel imager: magnitude and effects of x-ray scatter. Med Phys. 2001;28:220-31. cross ref
13. Ludlow JB, Davies-Ludlow LE, Brooks SL, Howerton WB. Dosimetry of 3 CBCT devices for oral and maxillofacial radiology: CB Mercuray, NewTom 3G and i-CAT. Dentomaxillofac Radiol. 2006;35:219-26. cross ref
14. Kim HJ, Friedman EM, Sulek M, Duncan NO, McCluggage C. Paranasal sinus development in chronic sinusitis, cystic fibrosis, and normal comparison population: a computerized tomography correlation study. Am J Rhinol. 1997;11:275-81. cross ref
15. Chiu AG. Osteitis in chronic rhinosinusitis. Otolaryngol Clin North Am. 2005;38:1237-42. cross ref